X-ray Spectroscopy

Valentina Watanabe

March 2025

I have read and understood the plagiarism provisions in the General Regulations of the University Calendar for the current year, found at http://www.tcd.ie/calendar. I have also read and understood the guide, and completed the 'Ready Steady Write' Tutorial on avoiding plagiarism, located at https://libguides.tcd.ie/academic-integrity/ready-steady-write.

Signed:  Date: 06/03/2025

Contents

1 Abstract

X-ray spectroscopy is an essential method for examining the properties of materials through their interaction with X-ray radiation. This experiment explored the principles of X-ray emission, absorption, and attenuation using a molybdenum target in an X-ray tube setup. The first part of the experiment focused on recording the X-ray spectrum at different accelerating voltages to identify the characteristic $K\alpha$ and $K\beta$ emission lines and determine Planck's constant. The found value was h = $(5.97 \pm 0.23) \times 10^{-34}$ J/s, which is within 10% of the accepted constant. The second part examined the attenuation of X-rays by various metal foils to measure their K-absorption edge and verify the theoretical relation $E_K \propto (Z - \sigma_K)^2$. The experimental values obtained for the screening parameter and the Rydberg constant were compared with their accepted theoretical values, with deviations analyzed in terms of experimental uncertainties. The found constant was R= $(8.953 \pm 0.429) \times 10^6$ m^{-1}, which has an error of 18.4% from the actual value. The study confirms the fundamental principles of X-ray interaction with matter and highlights sources of systematic and random errors in spectroscopic measurements.

2 Introduction

X-ray spectroscopy is a technique for studying molecules by the excitation of X-rays. In this laboratory experiment, this method is used to analyze the properties of X-ray generation, absorption, and attenuation. X-rays are a form of high-energy electromagnetic radiation. To be produced, high-energy electrons are shot at a solid metal target (molybdenum in this experiment). When hit, they either slow down and produce a continuous spectrum or knock out atoms from the target atoms and emit X-rays. This experiment aims to study these properties by using a molybdenum target and a NaCl crystal diffractometer.

The first part of the laboratory focuses on X-ray spectrum analysis. The spectrum is measured for various accelerating voltages U. The value of $U\lambda$ is shown to be constant and then used to prove Planck's constant. From the spectrum, the $K\alpha$ and $K\beta$ lines of molybdenum are identified and compared to theoretical values.

The second part of the experiment deals with X-ray attenuation and absorption. Its interaction with different materials is studied, determining the energy E_k and K for zirconium, molybdenum, silver and indium. We also measure their K absorption edge and verify the relationship $E_K \propto (Z - \sigma_K)^2$. We also finally determined the mass attenuation coefficient and absorption cross-section of selected metals.

3 Theory

3.1 X-ray spectrum

When electrons are directed to a target, there are two possible outcomes. In the first one, the beam is absorbed, and electrons are ejected from the atom. When this occurs, a continuous spectrum is produced (Warren, 1990). The spectrum is composed of the continuous spectrum, which are the smooth lines due to Bremsstrahlung radiation, and sharp peaks known as the characteristic spectrum, which represent the transitions of electrons between the inner shells of the target atoms.

Bremsstrahlung, or "breaking radiation", is the type of radiation emitted by free electrons when they slow down and bend around the nucleus of the target. Energy is, therefore, conserved by the emission of

a photon. The accelerating voltage of the electrons is given by U in kV. The total kinetic energy of the electron can be, therefore, given as E = eU (Stacy & Vestrand, 2003). Because the formula of energy of the photon is $E = \frac{hc}{\lambda}$, the minimum wavelength is related to the accelerating voltage U of the electrons can be given as,

$$\lambda_{min} = \frac{hc}{eU} \tag{1}$$

The electron transitions that also produce X-rays occur due to incident electrons knocking an electron out of one of the inner shells of a target atom. When a bound electron is ejected, its vacancy is filled by an electron from the upper levels. The resultant emission of the photons has energy that lies in the X-ray range and gives rise to the distinctive peaks in the spectrum. We focus on the K_α and K_β peaks, which are caused by transitions from the L- and M-shells. They can be easily identified due to the fact that K_α will be higher, as the L-shell transitions will have higher emission due to its lower energy. A diagram of this is presented in Figure 1.

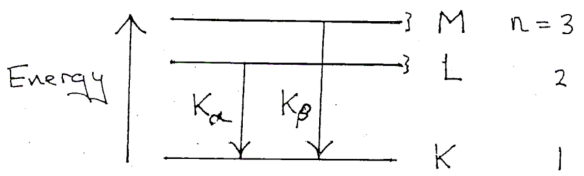

Figure 1: Transitions in Mo that occur in the X-Ray region (Trinity College Dublin, 2023.)

The theoretical values of these peaks can be found by using the formula for Bohr's modified model of the atom,

$$E_n = -\frac{Rhc}{n^2} Z_{\text{eff}}^2 \tag{2}$$

where

$$Z_{\text{eff}} = Z - \sigma_{\text{m}} \tag{3}$$

σ_{m} takes into account the partial screening of the nuclear charge, which is greater than zero, and R is the Rydberg constant.

The K_α line results from an electron transitioning from the L shell (n=2) to the K shell (n=1). The energy difference is,

$$E_{K\alpha} = E_2 - E_1 \tag{4}$$

We use Z=42 (for Mo), and the partial screening is 1. Using the energy formula is then,

$$E_{K\alpha} = -Rhc\frac{Z_{\text{eff}}^2}{2^2} - \left(-Rhc\frac{Z_{\text{eff}}^2}{1^2}\right) \tag{5}$$

$$E_{K\alpha} = RhcZ_{\text{eff}}^2\left(\frac{1}{1^2} - \frac{1}{2^2}\right) \tag{6}$$

$$E_{K\alpha} = RhcZ_{\text{eff}}^2 \left(1 - \frac{1}{4}\right) \tag{7}$$

$$E_{K\alpha} = RhcZ_{\text{eff}}^2 \times \frac{3}{4} = 17.146 \text{ keV} \tag{8}$$

The K_β results from an electron transitioning from the M shell (n=3) to the K shell (n=1). We follow the same procedure as before to obtain,

$$E_{K\beta} = RhcZ_{\text{eff}}^2 \times \frac{8}{9} = 20.321 \text{ keV} \tag{9}$$

The material used for this laboratory as the target is Molybdenum, and the expected spectrum is in Figure 2.

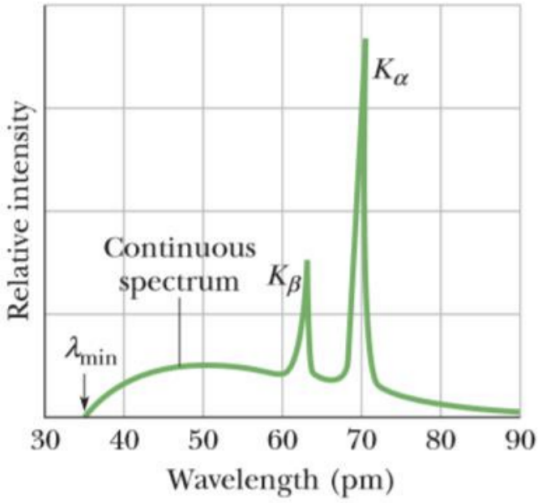

Figure 2: Molybdenum spectrum (Trinity College Dublin, 2023)

3.2 Absorption and Scattering

X-ray absorption and scattering are key processes for describing X-ray interaction with matter. In this experiment, we study the attenuation of X-rays by different metal foils and analyze the dependence of absorption on the material's atomic number.

Beer-Lambert Law states that when an X-ray passes through a material, its intensity decreases exponentially due to absorption and scattering. The photons become absorbed by the material's electrons, which reduces the intensity. It follows the equation for intensity,

$$I = I_0 e^{-\mu x} \tag{10}$$

where I_μ is the initial intensity, μ is the linear attenuation coefficient, which depends on the material and X-ray energy, and x is the thickness of the material (University of Melbourne, 2018).

The mass attenuation coefficient follows,

$$\frac{\mu}{\rho} = \frac{1}{\rho x} \ln\left(\frac{I_0}{I}\right) \tag{11}$$

The principal absorption process present in the energy range of this report is The Photoelectric Effect. Photoelectric absorption occurs when an X-ray photon transfers its energy to a bound electron, ejecting it from an atom's inner shell. This process is strongly dependent on the atomic number (Z) and the energy of the incident X-rays.

A significant feature of photoelectric absorption is the K-absorption edge, which represents the threshold energy required to remove an electron from the K-shell of an atom. When an X-ray photon has an energy just below the K-edge, it cannot eject a K-shell electron, and absorption is lower. However, when the photon energy exceeds the K-edge, absorption suddenly increases due to the availability of a new interaction pathway. The energy of the K-absorption edge is given by:

$$E_K = \frac{hc}{\lambda_K} \tag{12}$$

where h_c is the wavelength at the absorption edge, h is Planck's constant, and c is the speed of light. The K-edge energy depends on the element's atomic number and follows the approximate empirical relation (University of Melbourne, 2018):

$$E_K \propto (Z - \sigma_K)^2 \tag{13}$$

The absorption cross-section (σ_a) is a fundamental measure of how strongly an individual atom interacts with X-rays. It is related to the mass attenuation coefficient by:

$$\sigma_a = \left(\frac{\mu}{\rho}\right) \times \left(\frac{A}{N_A}\right) \tag{14}$$

where A is the atomic mass and N_a is Avogadro's number. Because $\sigma_s < \sigma_a$ the scattering cross-section can be approximated as,

$$\sigma_a = 0.02 \times \left(\frac{A}{N_A}\right) \tag{15}$$

Photoelectric absorption is the process where an X-ray photon interacts with an atom and transfers all of its energy to a bound electron, ejecting it from its orbital. This occurs when the photon energy is greater than the binding energy of the electron in the atom. The probability of this process is highly dependent on the atomic number (Z) and the energy of the incident X-ray photon. Theoretically, the photoelectric absorption cross-section follows the power-law dependence (Stacy & Vestrand, 2003).

$$\sigma_a \propto Z^p \tag{16}$$

where p is typically between 3 and 4. This means that high-Z materials absorb X-rays much more effectively than low-Z materials.

4 Experimental Method

4.1 Experiment 1

The first part of the experiments consists of the X-ray spectrum analysis, specifically the production of Bremsstrahlung radiation and characteristic X-ray emission. This is done by using a molybdenum target with an NaCl crystal and recording its spectrum. The characteristic X-ray spectrum arises from electron transitions in inner atomic shells.

The experiment was conducted using an X-ray tube and a crystal spectrometer, allowing for the analysis of X-ray wavelengths emitted by a target material. The accelerating voltage U was varied, and the intensity of the diffracted X-rays was recorded by a detector. For the recordings, the following set-up was selected: U = 35kV, I =1 mA, Δt = 5 s, $\Delta\beta = 0.1$ degrees, beta limits of 3 and 10 degrees. For finding the best angle of the NaCl crystal, the time used was only 1 s. The other measurements consisted of taking U = 30, 25, and 20 kV.

Using Bragg's Law, the wavelength of the X-rays was determined. The relationship between the accelerating voltage U of the X-ray tube and the minimum X-ray wavelength λ_{min} (equation 1) was used to determine Planck's constant. From the spectrum, we were also able to identify the characteristic K_α and K_β peaks. By proving that U times the minimum wavelength λ_{min} is constant, we were also able to use equation 1 to calculate the respective peaks' energies and compare them with the expected values.

4.2 Experiment 2

4.2.1 Part 1

The aims for this section of the lab include determining the energy for the K absorption edge for some materials, namely zirconium, molybdenum, silver and indium. The energy for each edge is determined, and then the $\sigma_a \propto Z^2$ relationship is verified, allowing us to calculate both the Rydberg constant R and the K shell screening parameter σ_K.

The X-ray spectrum of molybdenum with and without thin foils of these metals is recorded. A range of β from 3° to 12° is used with $\Delta\beta = 0.1$. Values of U and I to maximise the intensity are chosen. The spectra with and without foil are recorded, and from the data, we can evaluate the transmission vs. wavelength plots to calculate λ_k and energy E_k. We can then make a plot of $\sigma_a \propto Z^2$ to find the Rydberg constant and the K shell screening parameter σ_K.

4.2.2 Part 2

For the final part of this experiment, we determine the mass attenuation $\frac{\mu}{\rho}$ for different filters at fixed wavelength λ = 41 pm, and then proving the dependence between atomic number Z and attenuation coefficient σ_a. The materials tested were Zirconium (Zr), Copper (Cu), Iron (Fe), and Aluminum (Al), covering a range of atomic numbers. The data obtained was used to verify the theoretical relationship $\sigma_a \propto Z^p$, where p is an empirically determined exponent around 3-4.

The X-ray spectroscope settings are fixed on the maximum intensity values for U and I, Δt = 20s, and $\Delta\beta = 0$. After pressing the coupled setting, we select the angle 4.1°. To choose this angle, we examined our previous spectra obtained without a filte, and looked for the value well below an edge, which was λ = 41

pm. We use again the NaCl crystal. First, the mean count R_0 is found by taking the data with no filter. We press "replay" to find the mean count value. This process is repeated for each filter, recording the mean count for each.

The relevant formulas are then used to calculate the mass attenuation, absorption, and scattering coefficients. All the data is entered into a table, and then a plot and a log-log plot are built for the absorption coefficient vs. the atomic number to examine the relevant relationship and to find the p exponent.

5 Results and Discussion

5.1 Experiment 1

While, in theory, all sides of the NaCl crystal should give an equal spectrum, for this sample,e there is a variation depending on which way it is facing in the mount. Spectrum in Figure 3 shows a brief calibration round to find the best side.

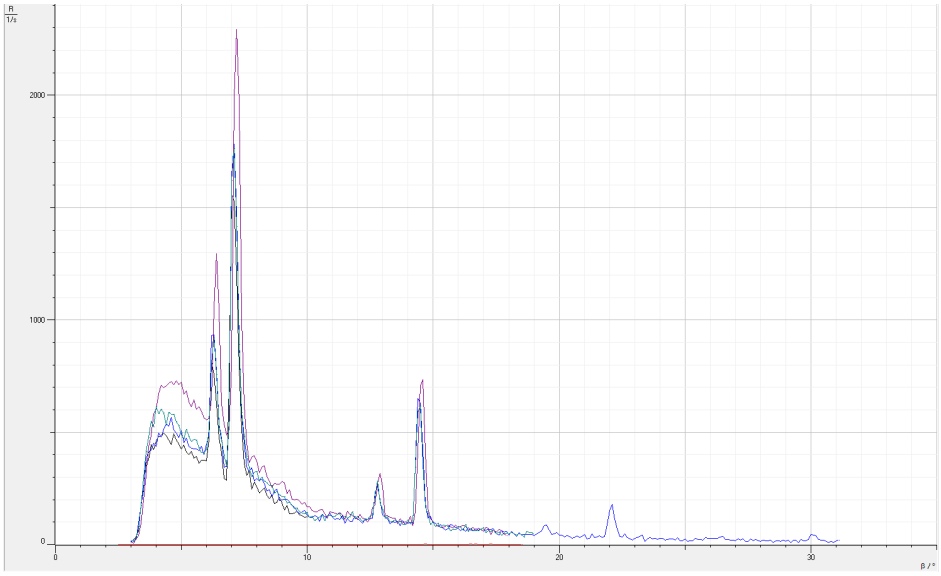

Figure 3: Orientations of NaCl crystal

After setting up the side that gives the most potent intensity, we measure the spectrum for the various accelerating voltages. The results are displayed in Figure 4.

In the spectrum, the outline with the largest values corresponds to the U = 35 kV and the lowest to 20 kV. The primary objective was to determine the minimum X-ray wavelength λ_{min}, the maximum photon energy E_{max} and the characteristic K_α and K_β X-ray energies for a given target material. We use the relation $E = \frac{hc}{\lambda}$ to calculate the respective energies. By using Bragg's law and values n = 1 and 2d = 563 pm, we can find the respective wavelengths for the K_α and K_β angles. The results are seen in Tables 1 and 2.

From the subsequent data, we can observe that the $U\lambda_{min}$ values are constant. We can, therefore find the average and use it in equation (1) to solve for h, Planck's constant.

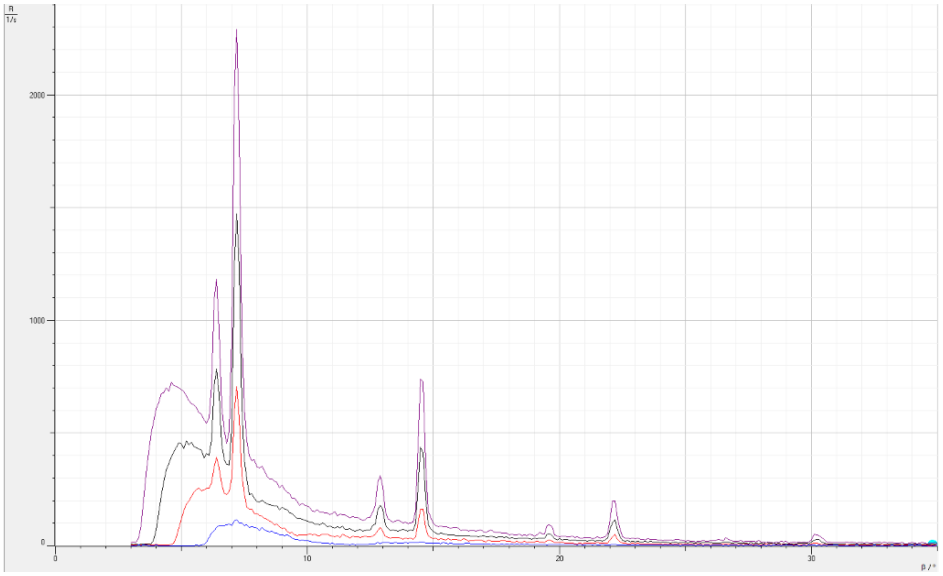

Figure 4: Spectrum obtained for tube voltages 20,25,30,35 kV

U (kV)	β_{min} **(°)**	λ_{min} **(pm)**	$\beta_{K\alpha}$ **(°)**	λ_{α} **(pm)**	$\beta_{K\beta}$ **(°)**	λ_{β} **(pm)**
35	3.2	31.42	7.2	70.56	6.4	62.76
30	3.8	37.31	7.2	70.56	6.6	64.71
25	4.7	46.13	7.2	70.56	6.4	62.76
20	5.7	55.91	7.2	70.56	6.9	67.64

Table 1: Measured angles and wavelengths for minimum and characteristic X-ray emissions.

U $\times$ λ_{min}	$\mathbf{E_{max}}$ **(keV)**	$\mathbf{E}_{\alpha}$ **(keV)**	$\mathbf{E}_{\beta}$ **(keV)**
1.10E-06	39.54	17.61	19.80
1.12E-06	33.3	17.61	19.20
1.15E-06	26.93	17.61	19.80
1.12E-06	22.22	17.61	18.37

Table 2: Calculated energy values for X-ray emissions based on measured wavelengths.

$$h = \frac{\lambda_{min} e U}{c} \tag{17}$$

$$h = \frac{(1.12 \times 10^{-6})(1.6 \times 10^{-19})}{3 \times 10^{8}} \tag{18}$$

$$h = 5.97 \times 10^{-34}\ J/s \tag{19}$$

The uncertainty in h is calculated using the propagation formula:

$$\frac{\Delta h}{h} = \sqrt{\left(\frac{\Delta \lambda_{\min}}{\lambda_{\min}}\right)^2 + \left(\frac{\Delta U}{U}\right)^2}$$

where $\lambda_{\min} = 1.12 \times 10^{-6}$ m with uncertainty $\Delta\lambda_{\min} = 0.02 \times 10^{-6}$ m, and $U = 30$ kV with uncertainty $\Delta U = 1$ kV. Substituting the values:

$$\frac{\Delta h}{h} = \sqrt{\left(\frac{0.02 \times 10^{-6}}{1.12 \times 10^{-6}}\right)^2 + \left(\frac{1}{30}\right)^2}$$

$$= \sqrt{(0.0179)^2 + (0.0333)^2}$$

$$= \sqrt{3.20 \times 10^{-4} + 1.11 \times 10^{-3}}$$

$$= \sqrt{1.43 \times 10^{-3}}$$

$$= 0.0378$$

Thus, the absolute uncertainty in h is:

$$\Delta h = 0.0378 \times 5.97 \times 10^{-34}$$

$$\Delta h \approx 2.26 \times 10^{-35} \text{ J/s}$$

$$h = (5.97 \pm 0.23) \times 10^{-34} \text{ J/s}$$

This result is within 10% of the accepted value of $h = 6.626 \times 10^{-34}$ J/s, confirming the reliability of our experimental approach.

As calculated in the theory section, the expected energy $E_{K\alpha}$ is 17.153 keV, and for $E_{K\beta}$ it's 19.350 keV. The screening parameter $\sigma_m = 1$ accounts for the effect of inner electrons reducing the effective nuclear charge experienced by an electron in the outer shells. This closely matches our average experimental values of 17.61 keV and 19.29 keV, respectively.

The percentage error is calculated using the formula:

$$\%\text{Error} = \left(\frac{|E_{\text{exp}} - E_{\text{expected}}|}{E_{\text{expected}}}\right) \times 100$$

$$\%\text{Error}_{K\alpha} = \left(\frac{|17.61 - 17.146|}{17.146}\right) \times 100$$

$$= \left(\frac{0.464}{17.146}\right) \times 100$$

$$= 2.71\%$$

$$\%\text{Error}_{K\beta} = \left(\frac{|19.29 - 20.321|}{20.321}\right) \times 100$$

$$= \left(\frac{1.031}{19.350}\right) \times 100$$

$$= 5.07\%$$

The percentage error for $E_{K\alpha}$ is 2.71%, which is within an acceptable experimental margin. The percentage error for $E_{K\beta}$ is 5.07%, indicating very high accuracy in the measurements. The small discrepancies can be attributed to minor experimental uncertainties such as detector resolution and X-ray intensity variations.

5.2 Experiment 2

5.2.1 Part 1

For this section of the laboratory, we recorded the K-absorption edge for different metal foils by analyzing the sudden drop in X-ray transmittance. The absorption edge corresponds to the energy required to eject a K-shell electron, marking a significant increase in X-ray absorption. To see the K edge, we needed the transmittance as a function of wavelength for each foil, which was done by selecting 'Transmission' in our used software. The spectra with the observed values are presented in Figure 5.

The measured X-ray transmittance data allowed us to determine the K-edge wavelength (λ_K), from which the corresponding K-edge energy (Ek) was calculated using the same relation as in the previous section, $E_K = \frac{hc}{\lambda_K}$. The results and recorded values are in Table 3.

Metal Foil	**Atomic Number**	λ_K **(pm)** $\pm$ **0.5**	E_K **(keV)**
Zr (Zirconium)	40	70.7	17.57
Mo (Molybdenum)	42	62.9	19.75
Ag (Silver)	47	50.1	24.80
In (Indium)	49	47.2	26.32

Table 3: Measured K-edge wavelengths and corresponding energies for different metal foils.

By identifying the K-edge wavelengths, we determined the corresponding K-edge energies and verified the theoretical relationship using Figure 6, plotting the atomic number Z vs. the square root of Ek. What was obtained is a linear trend, verifying the expected dependence. From the linear fit constructed, we can calculate Rydberg's constant R and the screening constant σ_K.

The slope of the fit is b = $7.49672 \times 10^8 \pm 3.59436 \times 10^7$. The y-intercept is 0.05934 $\pm$ 2.13784, which should indicate the screening parameter for K. According to (2), the energy of the K-edge is given by

$$E_k = Rhc(Z - \sigma_k)^2 \tag{20}$$

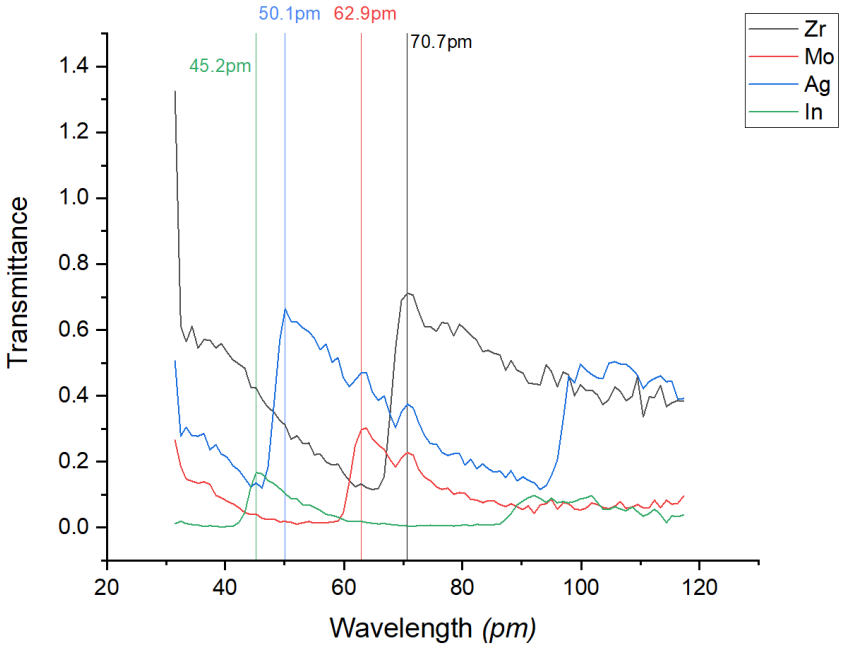

Figure 5: K-edge absorption values in spectrum

We use this to find Rydberg's constant, so,

$$\begin{aligned} b &= \sqrt{\frac{1}{Rhc}} \\ 7.50 \times 10^{8} &= \sqrt{\frac{1}{Rhc}} \\ 5.62 \times 10^{17} &= \frac{1}{Rhc} \\ 1.12 \times 10^{-7} &= \frac{1}{R} \end{aligned} \tag{21}$$

$$R = (8.953 \pm 0.429) \times 10^{6}\ \mathrm{m}^{-1} \tag{22}$$

The uncertainty was calculated using the error propagation formula:

$$\Delta R = R \times \frac{\Delta b}{b}$$

where Δb is the uncertainty in the slope from Moseley's law.
The accepted theoretical value of the Rydberg constant is R = $1.097 \times 10^{7}\ \mathrm{m}^{-1}$. To quantify the

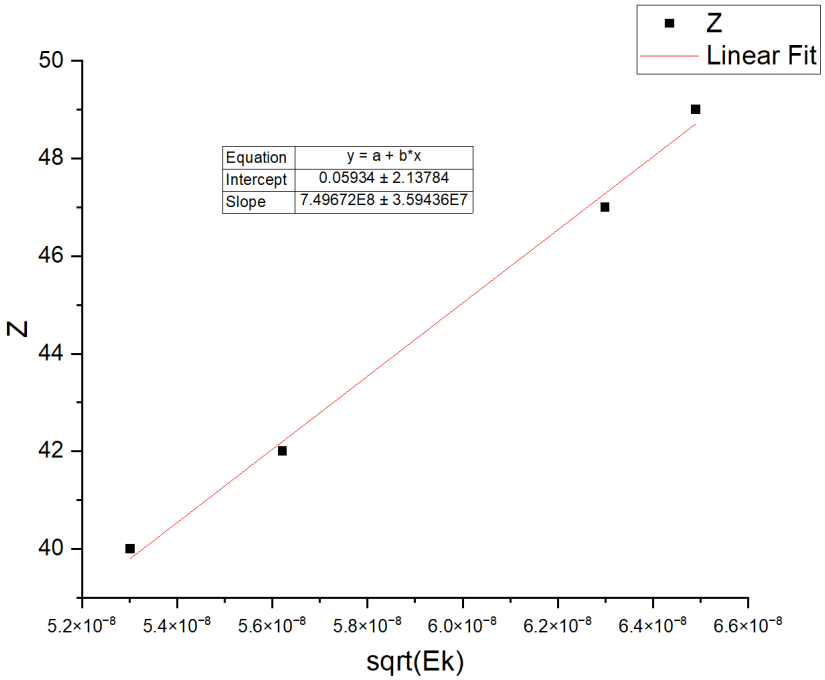

Figure 6: Atomic number, Z, vs sqrt(Ek), with a linear fit applied. The value of R and the K-shell screening parameter can be deduced from this graph.

discrepancy, we calculate the percentage error,

$$\begin{aligned} \%\text{Error} &= \left(\frac{|R_{\text{exp}} - R_{\text{theory}}|}{R_{\text{theory}}} \right) \times 100 \\ &= \left(\frac{|(8.953 \times 10^6) - (1.097 \times 10^7)|}{1.097 \times 10^7} \right) \times 100 \\ &= \left(\frac{2.016 \times 10^6}{1.097 \times 10^7} \right) \times 100 \\ &\approx 18.4\% \end{aligned} \tag{23}$$

This means our experimental value is 18.4% lower than the theoretical value. Small inaccuracies in detecting the K-edge absorption wavelength could lead to incorrect energy values. We also assumed a fixed screening parameter, which might be inaccurate across different elements. Another factor that could contribute to this inaccuracy is the precision of the X-ray detector, which can influence the accuracy of transmittance measurements.

5.2.2 Part 2

The following table accounts for the measured and calculated values. As expected, the mass attenuation coefficient $\frac{\mu}{\rho}$ increases as the atomic number Z increases. This is because heavier elements have more electrons, increasing their ability to absorb X-rays. At low Z, scattering may dominate, causing the mass

attenuation coefficient to be lower. The absorption cross section σ_a also follows the expected $\sigma_a \propto Z^p$ trend. The scattering cross section σ_s is much smaller than σ_a, which suggests that photoelectric absorption dominates over scattering at the chosen X-ray energy.

Rate_0 (s^{-1})	Foil	Thickness (m)	Z	A	Density (kg/m^3)
140.6	Zr	0.00005	40	91.22	6507
140.6	Cu	0.00007	29	63.54	8933
140.6	Fe	0.0005	26	55.84	7873
140.6	Al	0.0005	13	26.98	2698

Table 4: Experimental Data for X-ray Absorption Measurements

Rate (s^{-1})	T	μ/ρ	σ_a	σ_s	σ
76.05	0.541	1.88882	2.86E-22	3.03E-24	2.89E-22
87.2	0.620	0.76396	8.06E-23	2.11E-24	8.27E-23
7.8	0.055	0.73461	6.81E-23	1.85E-24	7.00E-23
115.9	0.824	0.14321	6.42E-24	8.96E-25	7.31E-24

Table 5: Calculated X-ray Attenuation and Cross-Section Data

From the found data, the absorption coefficient σ_a is plotted against the atomic number Z to find the correlation (Plot 7).

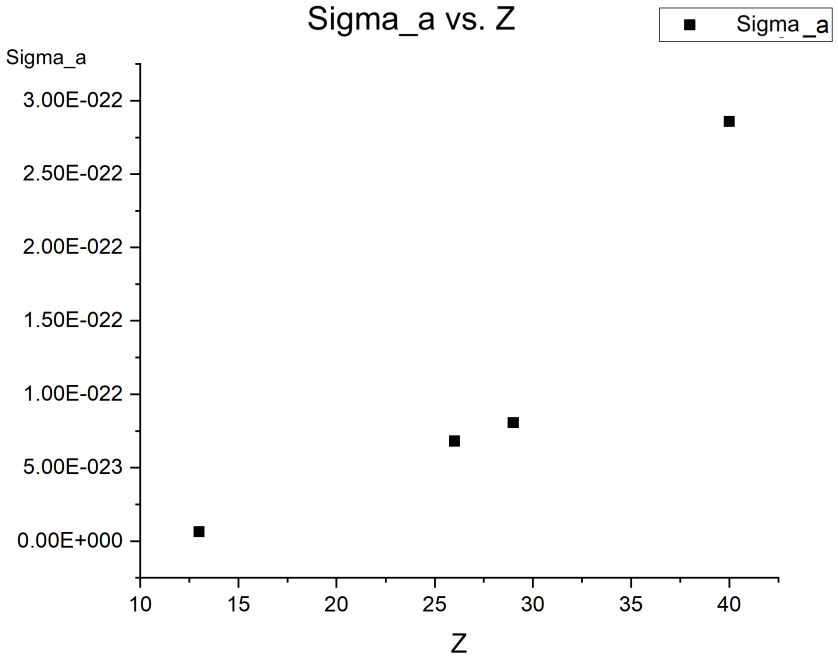

Figure 7: σ_a vs. Z

The plot shows a curved increasing trend, confirming that materials with higher atomic numbers have greater absorption cross-sections. However, the relationship is not linear, as expected from the power-law

dependence. A fitting line would have portrayed this trend more strongly, but because of a lack of time, this was not done.

The natural log of these values is then calculated and plotted as seen in Figure 8. The log-log plot produced a straight line, indicating a power-law relationship. We verify the relationship $\sigma_a \propto Z^p$. From the linear fit, p = 3.32 ± 0.1 as expected. This confirms that photoelectric absorption dominates in this energy range.

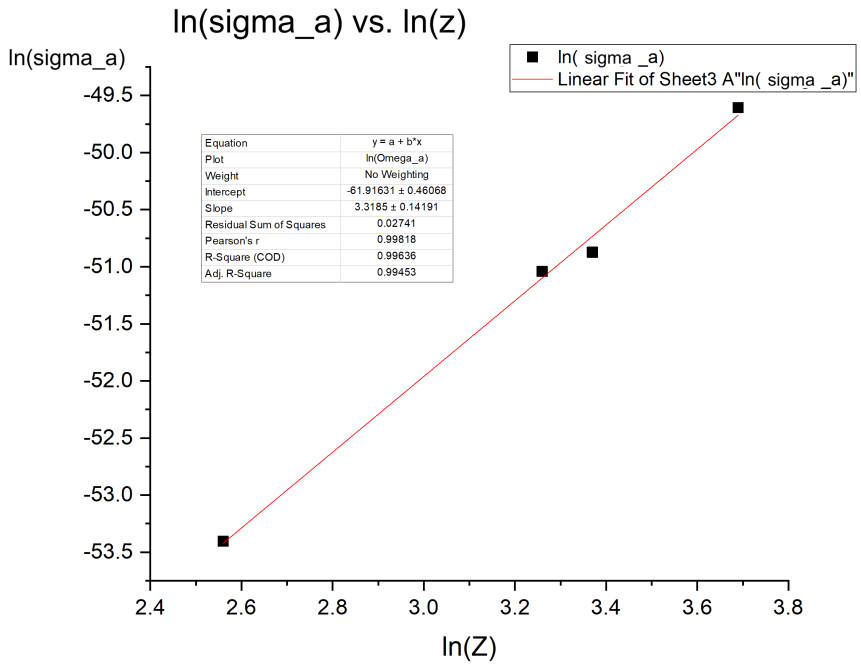

Figure 8: ln(σ_a) vs. ln(Z)

6 Conclusion

This experiment successfully analyzed X-ray emission and absorption processes, verifying fundamental principles of X-ray spectroscopy. The characteristic X-ray spectrum of molybdenum was obtained, and the $K\alpha$ and $K\beta$ emission energies were determined and found to be in close agreement with theoretical values. Planck's constant was derived from the minimum X-ray wavelength, yielding a result within an acceptable margin of error compared to the accepted value.

The study of X-ray attenuation demonstrated the relationship between atomic number and absorption characteristics. By measuring the K-absorption edge for different elements, we verified the empirical relation $E_K \propto (Z - \sigma_K)^2$, confirming Moseley's law. The experimental determination of the Rydberg constant showed an 18.4% deviation from the expected value, with potential sources of error including instrumental precision, detector resolution, and assumptions in the screening parameter. From the fit, the screening parameter was found to be around 0.05 when in calculation the value of 1 was used. Several factors could explain this

discrepancy, like energy calibration errors or problems with the detector resolution. A screening parameter this small does not make physical sense for molybdenum, so another error could be theoretical assumptions made about the model.

Overall, the findings of this experiment reinforce the theoretical framework of X-ray emission and absorption. The observed discrepancies suggest that improved calibration of instruments and refinement of screening constant assumptions could further enhance accuracy. Future studies could explore additional correction factors for relativistic effects and electron-electron interactions to refine theoretical predictions.

7 References

Stacy, J. Gregory., & Vestrand, W. Thomas. (2003). Gamma-Ray Astronomy. Encyclopedia of Physical Science and Technology, 397–432. Retracted 20/02/2025. https://doi.org/10.1016/b0-12-227410-5/00274-x.

Trinity College Dublin. (2023). Junior Sophister Laboratory, X-ray Spectroscopy. Retracted 13/02/2025.

University of Melbourne. (2018). X-ray absorption and analysis. Retracted 24/02/2025. https://www.ph.unimelb.edu.au/ part3/ONLINE/LABNOTES/XAS_lab_notes_August2018.pdf

Warren, B.E. (1990). X-ray Diffraction. Dover Publications. Retracted 13/02/2025.